Supplemental data for
Crystal structure of urea carboxylase provides insights into the carboxyltransfer reaction

Chen Fan[1], Chi-Yuan Chou[2], Liang Tong[3], Song Xiang[1*]

From the [1]Key Laboratory of Nutrition and Metabolism, Institute for Nutritional Sciences, Shanghai Institutes for Biological Sciences, Chinese Academy of Sciences, Shanghai 200031, P.R. China, the [2]Department of Life Sciences and Institute of Genome Sciences, National Yang-Ming University, Taipei 112, Taiwan, and the [3]Department of Biological Sciences, Columbia University, New York, NY 10027, USA

*Running title: *Crystal structure of urea carboxylase*

[*]To whom correspondence should be addressed: Key Laboratory of Nutrition and Metabolism, Institute for Nutritional Sciences, Shanghai Institutes for Biological Sciences, Chinese Academy of Sciences, Shanghai 200031, P.R. China. Tel: 86-21-54920495; Fax: 86-21-54920291; Email: sxiang@sibs.ac.cn.

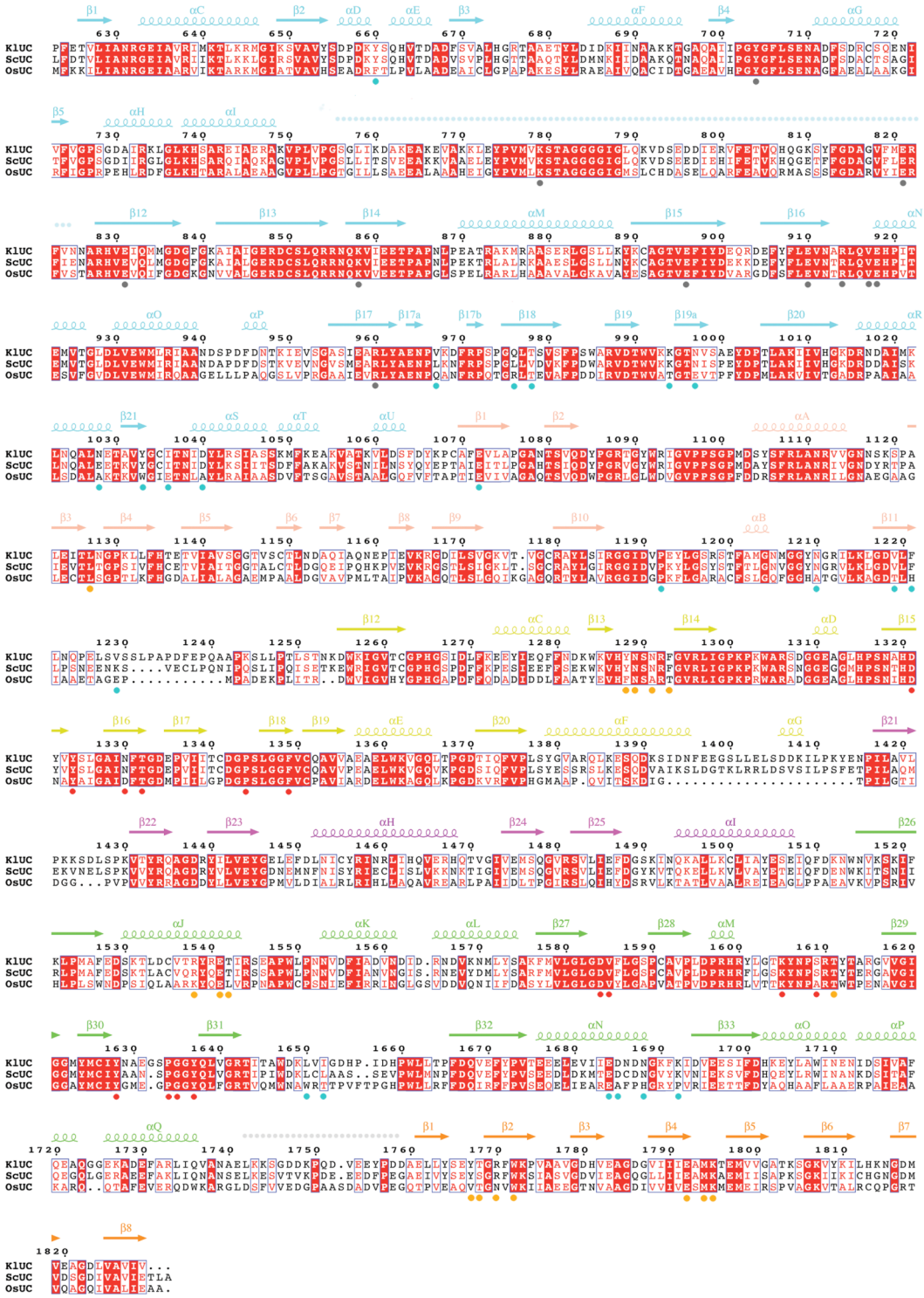

Supplemental figure S1. Sequence alignment of urea carboxylases. ScUC, UC domain of the *Saccharomyces cerevisiae* urea amidolyase; OsUC, the *Oleomonas sagaranensis* UC. Residue numbers and secondary structure elements are indicated for KlUC. Dots of different color indicate residues located in the active sites of the BC (gray) and the CT domains (red), and at the BC-CT (cyan) and the CT-BCCP (orange) interfaces. Disordered regions are indicated by dotted lines.

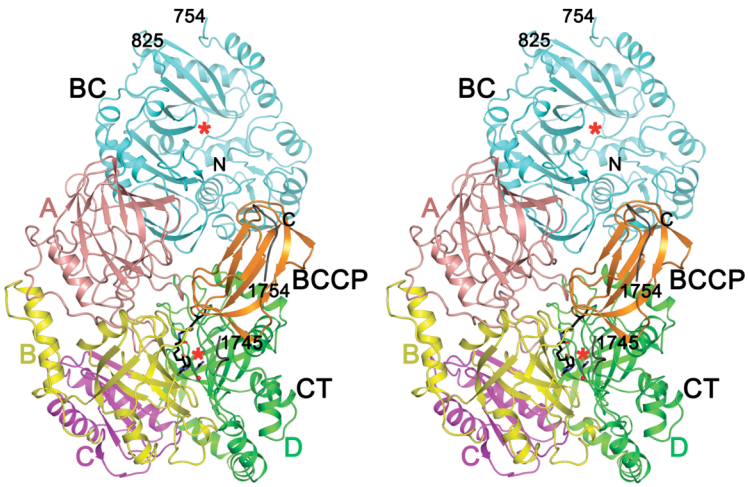

Supplemental figure S2. Stereo view of the KlUC structure. The biotinylated lysine (Lys1795), biotin, the urea and water molecules found at the CT domain active site are shown in stick and ball representations. The red stars indicate active sites of the BC and the CT domains.

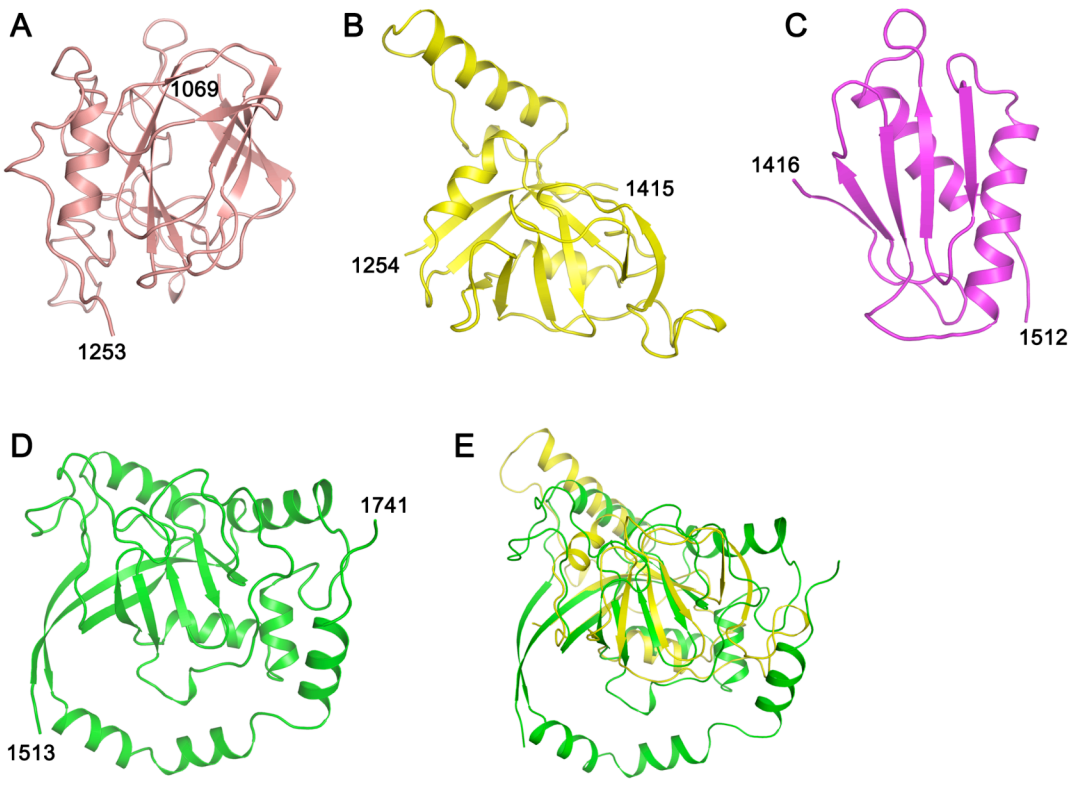

Supplemental figure S3. Structure of the KlUC CT sub-domains. (A)-(D) Structure of the KlUC CT sub-domains A-D. (E) Structure alignment of the KlUC CT sub-domains B and D.

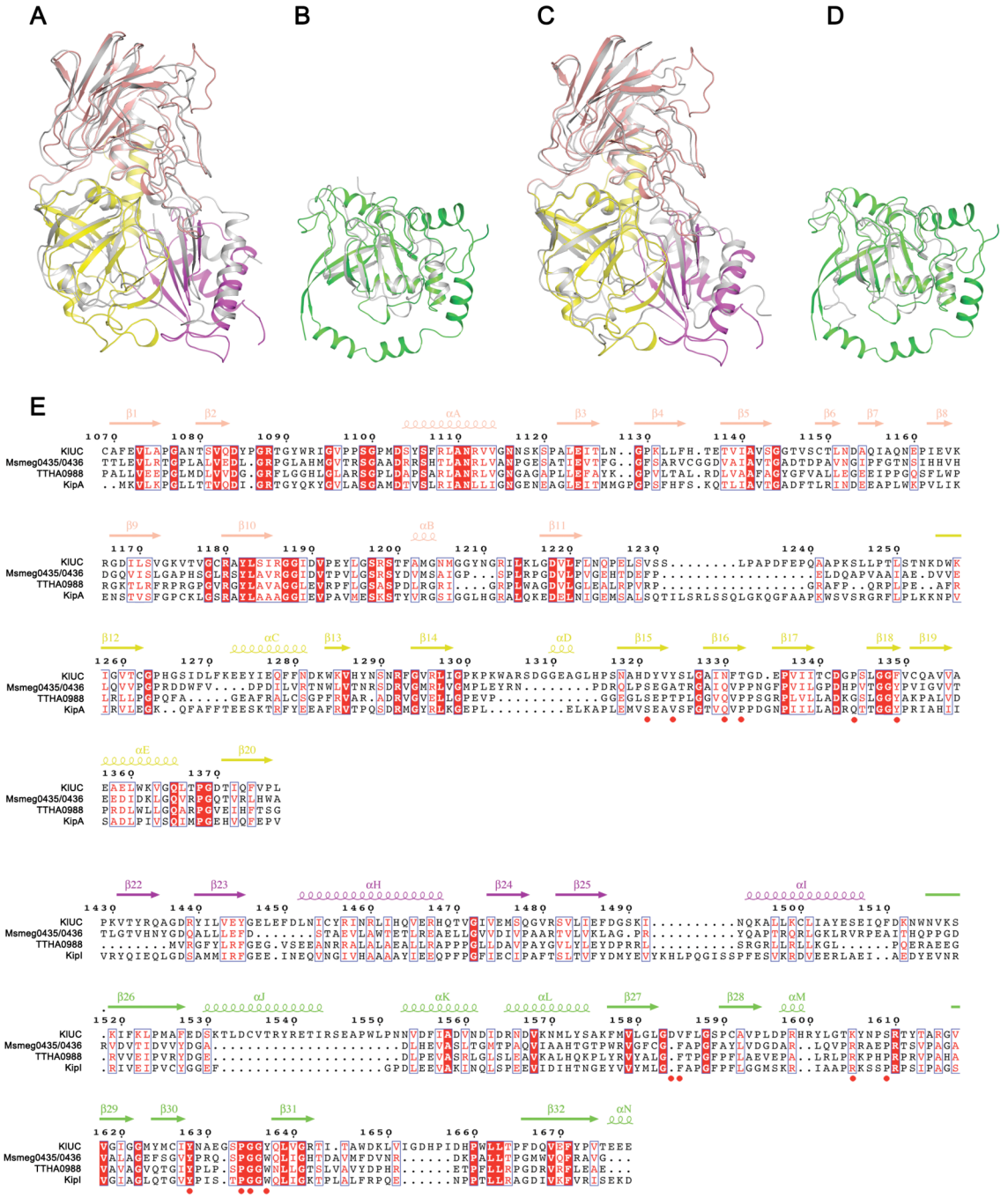

Supplemental figure S4. Structural homologues of the KlUC CT domain. (A) Structure alignment of the KlUC CT sub-domains A-C and their counterparts on TTHA0988 (PDB codes 3OPF and 3ORE, shown in gray). (B) Structure alignment of the KlUC CT sub-domain D and its counterpart on TTHA0988 (gray). (C) and (D) Same as panels (A) and (B), but for Msmeg0435/0436 (PDB code 3MML, shown in gray). (E) Sequence alignment of the KlUC CT domain and its structural homologues. Except for KipA, sequence alignments were based on alignments of structures, including structures of the KipI N- (PDB code 2KWA) and C- (PDB code 2ZP2) terminal domains. Residue numbers and secondary structure elements are indicated for KlUC. Red dots indicate important residues in the KlUC CT domain active site.

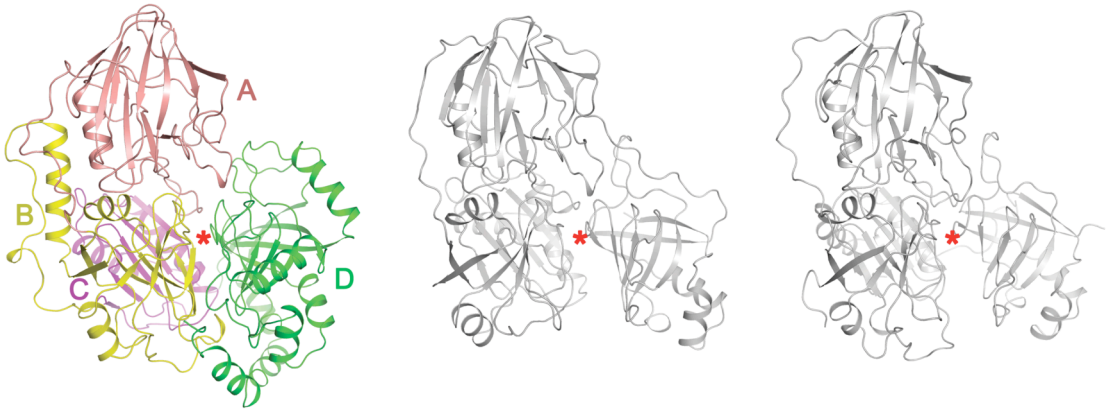

Supplemental figure S5. Structure of the KlUC CT domain and its homologues. Structures are aligned on the KlUC CT sub-domains A-C and counterparts in TTHA0988 (PDB codes 3OPF and 3ORE) and Msmeg0435/0436 (PDB code 3MML), and are shown side-by-side. The red stars indicate the cleft between the KlUC CT sub-domains B and D, and equivalent regions in TTHA0988 and Msmeg0435/0436.

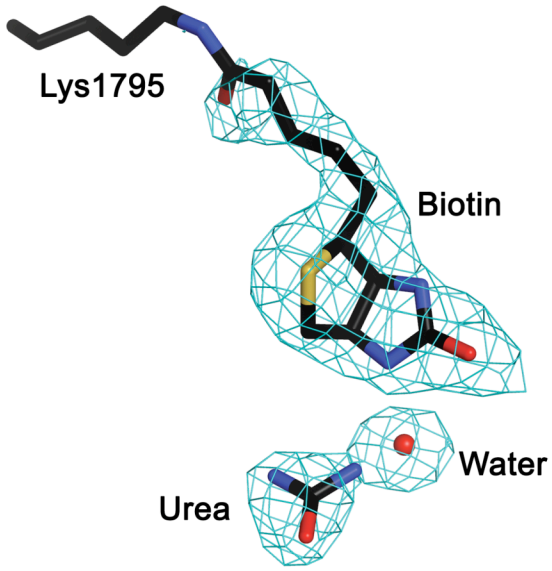

Supplemental figure S6. Difference density map of biotin and the urea molecule at the KlUC CT active site. Difference densities were calculated before biotin, the urea molecule and solvent atoms were included in the model, and are contoured at 3σ.

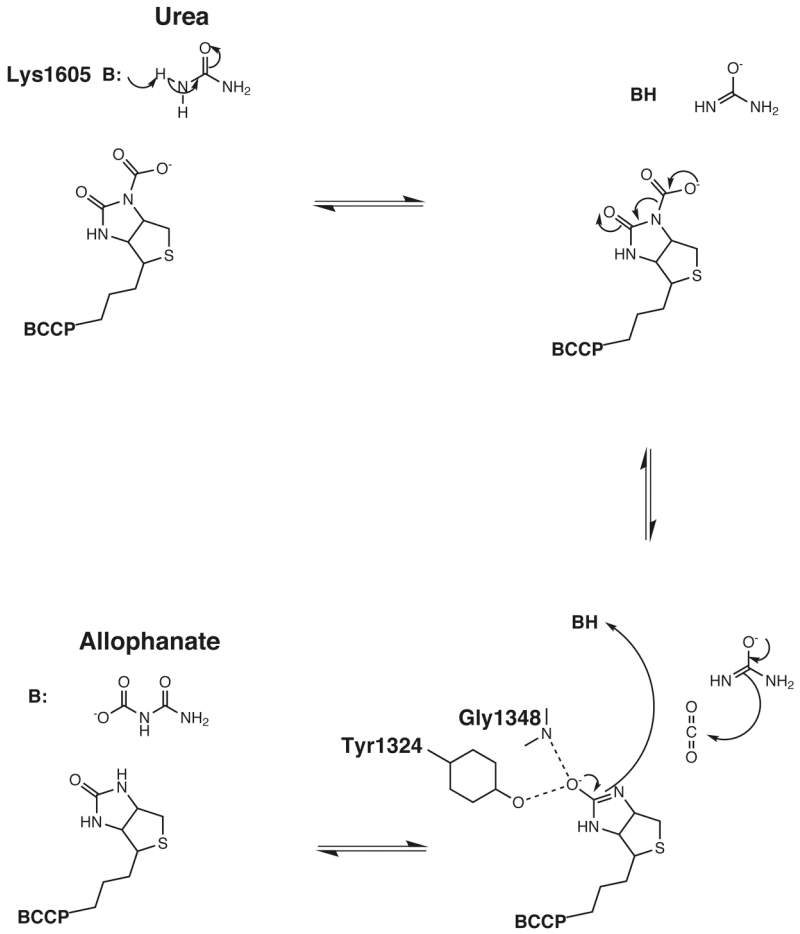

Supplemental figure S7. Schematic drawing of the carboxyltransfer reaction. The general base is represented by the letter B. Hydrogen bonds are represented by dashed lines.

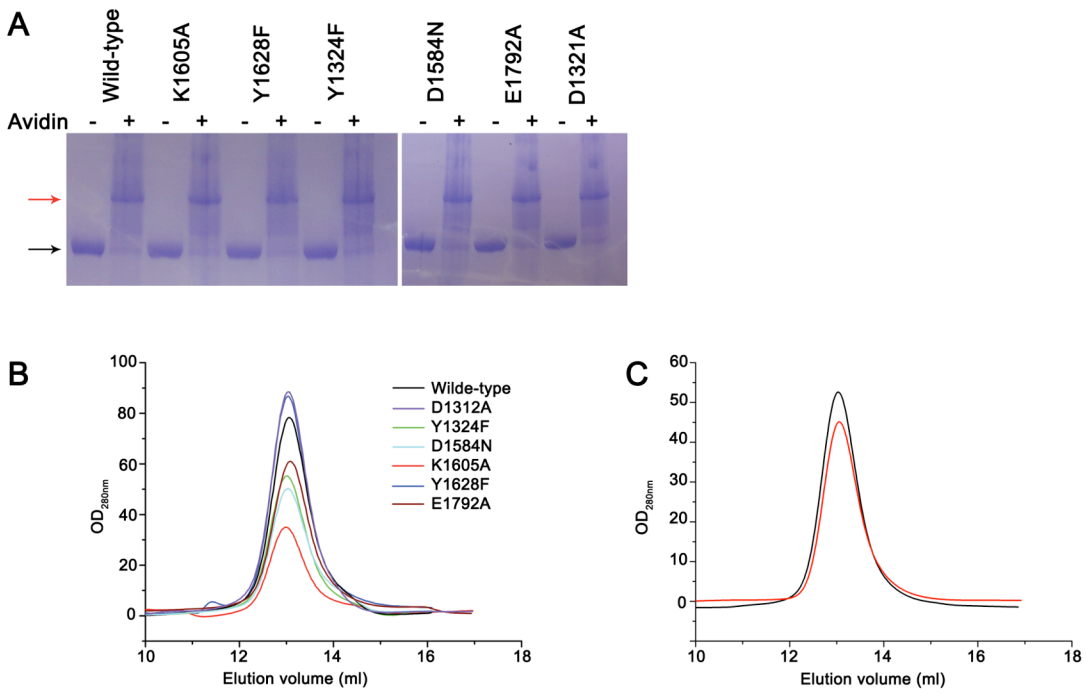

Supplemental figure S8. Characterization of the wild-type and mutant KlUC. (A) SDS PAGE analysis of KlUC. The black arrow indicates the molecular weight of KlUC. In the avidin + lanes, protein samples were denatured by boiling in the SDS loading buffer, incubated with 2 fold molar excess of avidin for 1 hour, before loaded to the gel. Avidin binding to biotinylated proteins caused a significant band shift towards higher molecular weight, indicated by the red arrow. (B) Gel-filtration analysis of KlUC. Purified wild-type and mutant KlUC were loaded on a superdex 200 10/30 column (GE healthcare), and eluted with a buffer containing 22 mM Tris/HCl pH 7.5 and 220 mM NaCl. (C) Same as (B), but for the wild-type KlUC with an elution buffer mimicking the buffer condition used in the activity assays (the red curve, the elution buffer contains 200 mM Tris/HCl pH8.0, 1 µM EGTA, 3 mM magnesium chloride, 19.5 mM potassium chloride, 200 mM sodium bicarbonate, and 18 mM urea). The experiment for the wild-type KlUC with an elution buffer described in (B) was repeated for reference (the black curve).

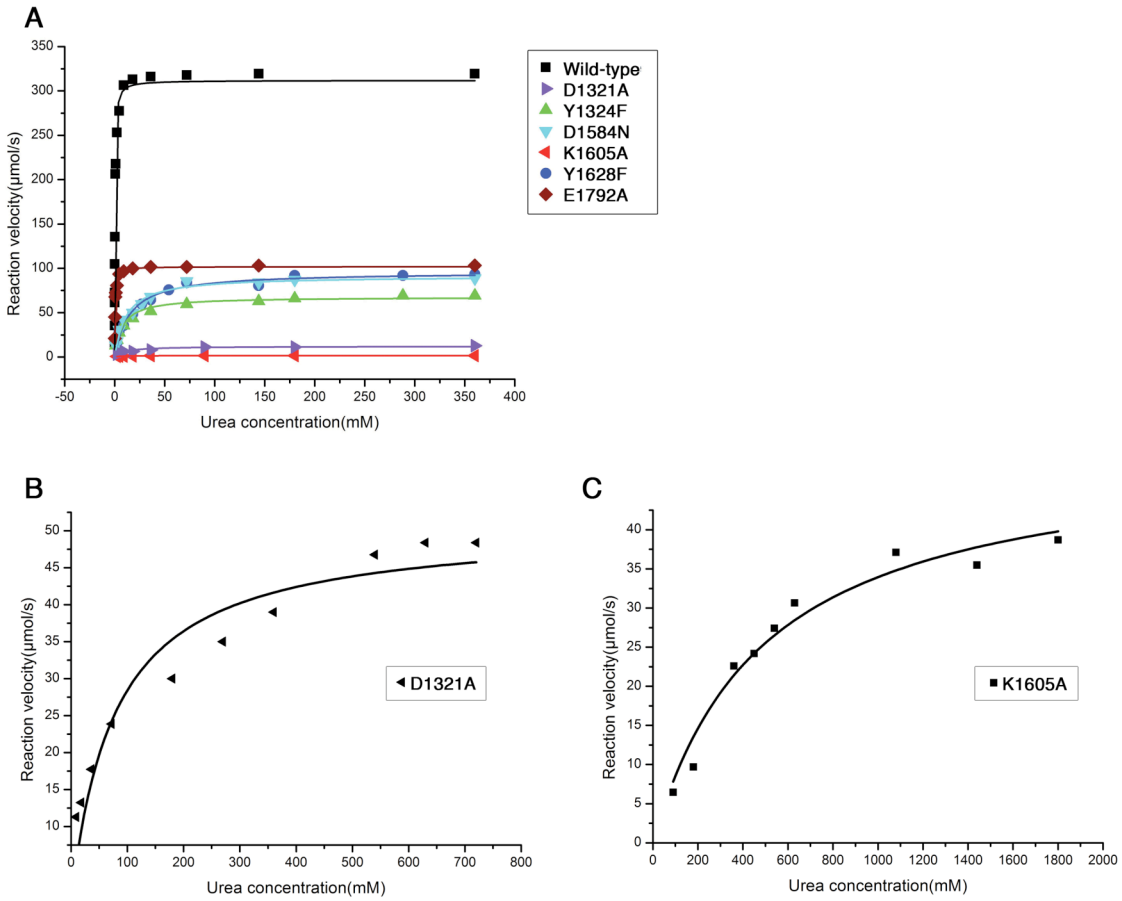

Supplemental figure S9. Activity measurements of the wild-type and mutant KlUC. (A) Activity measurements with 1.5 μM KlUC and 3.3 μM KlAH. (B) Activity measurements for the KlUC D1321A mutant, with 15 μM KlUC and 33 μM KlAH. (C) Activity measurements for the KlUC K1605A mutant, with 30 μM KlUC and 66 μM KlAH.